Bong Geun Chung
Jaebum Choo*

Department of Bionano Engineering, Hanyang University, Ansan, Korea

Received March 9, 2010
Revised June 4, 2010
Accepted June 6, 2010

Review

Microfluidic gradient platforms for controlling cellular behavior

Concentration gradients play an important role in controlling biological and pathological processes, such as metastasis, embryogenesis, axon guidance, and wound healing. Microfluidic devices fabricated by photo- and soft lithography techniques can manipulate the fluidic flow and diffusion profile to create biomolecular gradients in a temporal and spatial manner. Furthermore, microfluidic devices enable the control of cell-extracellular microenvironment interactions, including cell–cell, cell–matrix, and cell–soluble factor interaction. In this paper, we review the development of microfluidic-based gradient devices and highlight their biological applications.

Keywords:
Axon guidance / Chemotaxis / Gradient / Microfluidics / Stem cell differentiation
DOI 10.1002/elps.201000137

1 Introduction

Molecular gradients play a significant role in regulating biological and pathological processes, such as chemotaxis and embryogenesis [1–3]. Gradients have been employed for controlling cell growth, differentiation, migration, and apoptosis [4, 5]. Biomolecular gradients enable the control of pathological processes (*i.e.* chemotaxis) in a temporal and spatial manner [6, 7]. To control the cell–soluble factor interaction, conventional gradient-generators, such as the Boyden chamber [8], the Zigmond chamber [9], the Dunn chamber [10], and micropipette-based assay [11–14], have been previously developed.

The Boyden chamber has been used for studying chemotaxis [8]. This chamber is mainly consisted of upper compartment for cell seeding, lower compartment for chemoattractant solution, and porous membrane embedded between two compartments. Cells exposed to chemoattractant solution from lower compartment can migrate through the porous membrane. Although the motility of the cells exposed to chemoattractant solution is evaluated by using the Boyden chamber, major limitation of this assay is still remained, such as the inability to generate stable biomolecular gradients in a temporal and spatial manner. The Zigmond chamber [9] and Dunn chamber [10] have similar structures, consisting of two wells separated by a glass bridge. The concentration gradient was generated between a glass bridge and a coverslip, where cells were seeded. Despite their potential to study cell migration, these systems have the lack of maintaining steady-state gradients during longer-period culture time. A glass micropipette assay has also been used to regulate axon guidance [12, 13] and yeast polarization [14]. This micromanipulator-based assay can directly access to the cells and the pulsatile ejection of chemokines enables the generation of spatial gradients around a pipette. However, the equipment of this system is expensive and high-throughput experiments are difficult to be performed in a parallel manner.

Although these conventional gradient-generators have been used for studying chemotaxis and axon guidance, there are still many limitations, including the inability to maintain stable tempo-spatial gradients and the lack of the cell monitoring in a real-time manner. To overcome these limitations imposed by conventional gradient-generators, PDMS microfluidic-based gradient devices have been recently developed [15–21]. Microfluidic devices fabricated by photo and soft lithography techniques enable the manipulation of fluid flow, the generation of stable concentration gradient profiles, and real-time monitoring of the cells [2, 22–24]. Given these unique characteristics, microfluidic devices have been widely used for cell biology applications [24, 25]. In this paper, we review the recent development of gradient-generating microfluidic platforms (*i.e.* flow-based and diffusion-based gradient device) and their various biological applications, such as chemotaxis, stem cell differentiation, axon guidance, endothelial cell migration, and yeast mating.

Correspondence: Professor Bong Geun Chung, Department of Bionano Engineering, Hanyang University, Ansan 436-791, Korea
E-mail: bchung@hanyang.ac.kr
Fax: +82-31-436-8153

Abbreviations: EBs, embryoid bodies; **EGF,** epidermal growth factor; **MMP,** matrix metalloprotein; **MSCs,** mesenchymal stem cells; **VEGF,** vascular endothelial growth factor

*Additional correspondence: Professor Jaebum Choo
E-mail: jbchoo@hanyang.ac.kr

2 Microfluidic gradient devices

The flow-based and diffusion-based microfluidic platform is an enabling experimental tool to generate stable concentration gradients in a tempo-spatial manner and is a potentially powerful method for various biological applications (Table 1). To create this biomolecular gradient in a well-defined microenvironment, fluidic flow-based microfluidic gradient generator has been previously developed [26, 27].

2.1 Flow-based microfluidic gradient device

Flow-based microfluidic platforms enable the control of concentration gradients using laminar flow and diffusive mixing (Fig. 1A). These devices were consisted of the serpentine-based microchannel and cell culture area. In general, two or three solutions are mixed and splitted in a microchannel, resulting in generating stable concentration gradients in perpendicular to the flow direction. As compared with conventional well-plate culture methods that have used uniform concentrations of chemicals, we can rapidly generate various gradient profiles (*i.e.* single, overlapping, and dynamic switch gradient profile) in a single microfluidic device. Various profiles and steepness of concentration gradients can be generated in a single microfluidic device and the cocktail mixtures of soluble factors can be precisely delivered into each microchannel, resulting in performing high-throughput experiments. In particular, we can investigate the effect of autocrine and paracrine signaling on cell growth and differentiation in a flow-based microfluidic gradient device. Furthermore, the microfabrication process to create flow-based microfluidic devices is relatively straightforward. Despite these advantages, the flow-based microfluidic device has some limitations, such as the inability to maintain secreted molecules (*i.e.* autocrine, paracrine signaling), the lack of minimizing the shear stress, the inability to generate gradient profiles in a 3-D scaffold, and the lack of creating chaotic mixing (Fig. 1).

Recently, the flow-based rapid generation of long-range concentration gradients in a portable microfluidic device has been reported [28]. The portable microfluidic-based gradient device can be generated by using surface tension and passive pump technique that has been previously developed [29, 30]. The difference in the surface tension between larger and smaller reservoirs as well as the evaporation has been employed to deliver the solution into the microchannel without external syringe pumps. Briefly, the forward and backward flow derived from a passive pump and evaporation in a microfluidic device enables the generation of centimeter-long concentration gradients in a simple and rapid manner. Furthermore, a multi-purpose microfluidic system has been developed to create the combinatorial gradient profiles controlled by a binary multiplexer [31]. Various flow-based gradient patterns were generated by selecting chemical combinations of 16 inlet multiplexer controlled by a programmable Labview system. This microfluidic system that could create dynamic gradients might be useful for high-throughput screening applications. In addition to chemical gradients, multicomponent protein gradients have been generated by using the depletion effects in a flow-based microfluidic device [32]. The counterpropagating gradients of collagen and bovine serum albumin were created in a microfluidic channel for the immunoassay applications.

2.2 Diffusion-based microfluidic gradient device

Another approach for creating concentration gradients in a microfluidic device is to use pure diffusion through the membrane or hydrogel for generating diffusion-based gradients (Fig. 1B). As compared with the flow-based gradient-generating microfluidic device, diffusion-based microfluidic device has several advantages, such as shear stress is negligible, secreted molecule is maintained, and gradients can be generated in a 3-D scaffold. Despite these merits, the diffusion-based microfluidic device has the inability to generate rapid and dynamic gradient profiles. (Fig. 1).

The membrane-based gradient in a microfluidic device has been developed by using the diffusion on a 2-D surface [16]. The device was consisted of three PDMS layers, including top reservoir, middle sealing layer, and the microchannel in a bottom layer, which could connect between the source and sink region. The solution was diffused through the membrane (0.2 and 10 μm pore diameter) to create linear concentration gradients. As a proof-of-the concept, neutrophil chemotaxis was analyzed in a membrane-based microfluidic gradient device. Furthermore, a microfluidic multi-injector, which is a similar mechanism to conventional micropipette-based assay, has been developed to create soluble gradients [33]. This microfluidic multi-injector was developed by a multi-layer soft lithography technique. The pneumatically actuated microvalve enabled the release of solution (~130 pL) around the orifice to create the diffusion-based single and overlapping gradients. The steady-state radial gradient was generated within 10 min in a microfluidic multi-injector.

However, previous diffusion-based systems have generated simple gradients on a 2D surface. To create complex gradients in a 3-D environment, the diffusion-based gradient has been recently generated in a multi-layer microfluidic device containing hydrogels [19]. The molecules in two reservoirs were diffused through the hydrogel in the middle layer and molecular gradients containing complex shapes (*i.e.* W-shaped, steplike, and parabolic shape) were generated in a fluidic microchannel of the bottom PDMS layer. To date, the flow-based gradient generator has used the simple microchannel networks, whereas the diffusion-based gradient device has employed the multiple PDMS layers, embedding a membrane or hydrogel. Based on the principles for generating flow-based and diffusion-based chemical gradients, we review various

Table 1. Summary of the development of microfluidic-based gradient devices and their biological applications

Type	Biological applications	Research highlight	Ref.
Flow-based gradient	Neutrophil chemotaxis	IL-8, LTB4 overlapping gradient	[38]
		Dynamic IL-8 gradient	[39]
		Chemoattractant–receptor interaction	[40]
	Cancer chemotaxis	EGF gradient sensing of breast cancer cells	[47]
		EGF receptor-cell motility study	[51]
	Bacteria chemotaxis	Chemoeffector–receptor interaction	[18]
		Cell migration in a T-shaped microchannel	[59]
		E. coli behavior in response to competing attractant and repellent gradients	[60]
	Stem cell differentiation	Differentiation into astrocytes of human neural stem cells	[21]
		Growth and death of mouse neural stem cells	[68]
		Growth of human mesenchymal stem cells	[69]
		Neural progenitor cell-derived neurons in Shh/FGF8 and Shh/BMP4 gradients	[70]
	Axon guidance	Hippocampal neurons on substrate-bound gradients of laminin	[81]
		Growth cone behavior of chick retinal ganglion neurons in response to ephrinA5 gradients	[82]
	Endothelial cell migration	Cell migration in response to VEGF-A gradients	[86]
		Call attachment on PEG-RGDS gradients	[88]
	Yeast mating	*Saccharomyces cerevisiae* morphology by α–factor gradients	[94]
	Cytotoxicity	Cardiac toxin cytotoxicity of cardiac muscle cells	[28]
		Cadmium-induced cytotoxicity of fibroblasts	[98]
		Anti-cancer drug-induced apoptosis	[99]
Diffusion-based gradient	Neutrophil chemotaxis	Dynamic gradient-induced desensitization of human neutrophils	[41]
		Human neutrophils in EGF gradients of collagen gels	[42]
		CXCL8/IL-8 radial gradients	[43]
	Cancer chemotaxis	Cancer migration in response to EGF gradients	[42]
		FBS gradient-induced cell migration	[50]
		Cancer migration restrained by an MMP inhibitor	[52]
	Bacteria chemotaxis	*E. Coli* strain RP437 behavior in attractant and repellent gradients derived from membrane-based device	[56]
	Stem cell differentiation	Human embryonic stem cell culture on a membrane-based chip	[76]
	Endothelial cell migration	Capillary formation of human adult dermal endothelial cells in collagen gels	[90]
		Capillary growth in co-culture with cancer and endothelial cells	[91]
	Yeast mating	Mating pathway of *Saccharomyces cerevisiae*	[95]
	Cytotoxicity	Hepatocyte behavior in toxicant gradient of 3-D peptide scaffolds	[100]
		3-D hepatocyte chip for drug toxicity testing	[101]
		Cytotoxicity of murine hepatocytes encapsulated within 3-D agarose gel microchannels	[102]
Oxygen gradient	Bacteria growth	Bacteria growth in response to oxygen gradients	[61]
		Bacteria growth in multiplexed oxygen gradients	[62]
Mechanical stiffness gradient	Neurite outgrowth	Neurite length of chick dorsal root ganglia cells in 3-D genipin gradients	[85]
Material gradient	Endothelial cell attachment	Hyaluronic acid/gelatin gradients and endothelial cell gradients	[89]

biological applications (*i.e.* chemotaxis, stem cell differentiation, axon guidance, endothelial cell migration, and yeast mating) using current development of microfluidic-based gradient platforms on a 2-D surface and 3-D hydrogel microenvironment. In addition to chemical gradients, we review the material, oxygen, and mechanical stiffness gradients in a microfluidic device and also highlight their biological applications.

3 Biological applications

3.1 Neutrophil chemotaxis

Neutrophils, polymorphonuclear leukocytes, play an important role in controlling the immune system. They can roll and adhere to the endothelial surface in the mainstream of blood vessels [34, 35]. Cell rolling and adhesion are

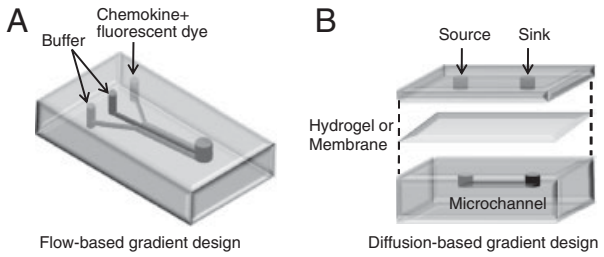

Figure 1. The schematic designs of flow-based and diffusion-based microfluidic gradient devices.

significantly dependent on the leukocyte selectin (P-, L-, and E-selectin), integrin ligand (*i.e.* intercellular adhesion molecule-1 (ICAM-1)), and pro-inflammatory molecules (*i.e.* n-formyl-Met-Leu-Phe (fMLP)) presented on the endothelial surface [34]. Neutrophils exposed to chemoattractant gradients from the infection or inflammatory sites can also migrate through the interstitial tissues [34, 35]. This directed cell migration of an immune cell in response to chemokine gradients is called chemotaxis [36].

The flow-based microfluidic devices containing serpentine microchannels have been previously used to study neutrophil chemotaxis [15, 37]. Various gradient profiles (*i.e.* linear, cliff, and hill-type gradient) were generated in a serpentine-based microchannel. Neutrophils exposed to chemoattractant gradients of interleukin-8 (IL-8) migrated toward higher concentrations of IL-8. Neutrophils were tracked in a real-time manner and their migration speed and chemotactic index were also analyzed. Furthermore, neutrophils can respond to complex opposite gradients. The opposite gradients of chemoattractants (*i.e.* IL-8, Leukotriene B_4 (LTB_4)) have been used to study neutrophil chemotaxis [38]. In an opposite gradient of IL-8 and LTB_4, neutrophils were less migrated toward higher concentration of IL-8 as compared with single linear gradient of IL-8. The linear gradient of IL-8 also showed more effective chemoattractant effect than that of LTB_4. Furthermore, a flow-based microfabricated platform that can rapidly switch chemical gradients of IL-8 has been developed to control neutrophil chemotaxis [39]. This device that was consisted of PDMS membrane and metal valve enabled the control of neutrophil motility. The quantitative analysis showed that the cells exposed to IL-8 gradients migrated toward higher concentration of IL-8; however, when the direction of gradients was changed, neutrophils exposed to opposite gradients were moved toward the opposite direction of the gradient. The migration mechanism of neutrophils exposed to dynamic chemokine gradients was that, as the direction of chemokine gradients was changed, neutrophil migration was stopped and neutrophils were subsequently depolarized. After then, neutrophils were polarized again, resulting in migration into the reverse direction. Therefore, it was revealed that the polarization (actin acts as a leading edge in a cytoskeletal model) and depolarization process played an important role in controlling neutrophil migration. Another study suggested that microtubules (structural cytoskeleton component in a cell) within the neutrophils were important for controlling cell polarization and gradient sensing [40]. The experimental and analytical approach demonstrated the hypothesis of adaptive-control model for neutrophil polarization, showing that the protrusion was grown toward the direction of chemokine gradients and protrusion activity was obtained through local stabilization of microtubules. It has also been shown that chemoattractants enabled the control of local stabilization of microtubules that could significantly affect neutrophil polarization. Therefore, local stabilization of microtubule from cellular periphery played an important role in understanding the neutrophil polarization process.

To study gradient-induced desensitization of human neutrophils, the open-chamber microject device has been used to create dynamic gradients without applying the fluidic flow (Fig. 2A) [41]. The gradient-induced desensitization was performed by using five stages, such as random, CXCL8 chemoattractant gradient, CXCL8 gradient shift, exchange soluble factors, and fMLF chemoattractant gradient at opposite direction. The quantitative analysis showed that neutrophils were responded to two dynamic chemoattractant gradients, showing that cell migration velocity was increased in CXCL8 gradients, but it was decreased in fMLF gradients. Another diffusion-based microfluidic device containing sink-source microchannels has been used to generate linear and non-linear gradients of hydrogels in a well-defined 3-D microenvironment [42]. The bridge microchannel of an ''H''-shaped microfluidic device has two different channel morphologies, such as straight and curvature shape, to control linear and non-linear gradients. The migration of human neutrophils exposed to epidermal growth factor (EGF) gradients in a 3-D collagen gel was monitored and their chemotactic effects were analyzed. The microvalve-based chemotaxis platform that can release the chemoattractants to generate radial gradients in a diffusion manner has also been developed to study neutrophil chemotaxis [43]. CXCL8 is a member of CXC family of chemokines. Cells were exposed to CXCL8/IL-8 radial gradients and their migration behavior was investigated in a microfluidic device. It has been shown that neutrophils directly migrated toward CXCL8 gradients (~200 ng/mL), whereas neutrophils exposed to higher concentrations (200–400 ng/mL) of CXCL8 gradients showed chemokinesis (random migration). From this approach, concentrations of CXCL8 gradients that could switch neutrophil chemotaxis to chemokinesis were identified. Therefore, microfluidic gradient platforms that create various shapes of gradient profiles can be useful for understanding the mechanism of neutrophil chemotaxis.

3.2 Cancer chemotaxis

Understanding of metastasis mechanism plays a significant role in treating tumor cells, because metastasis has been found in the late stage of cancer disease. There are two

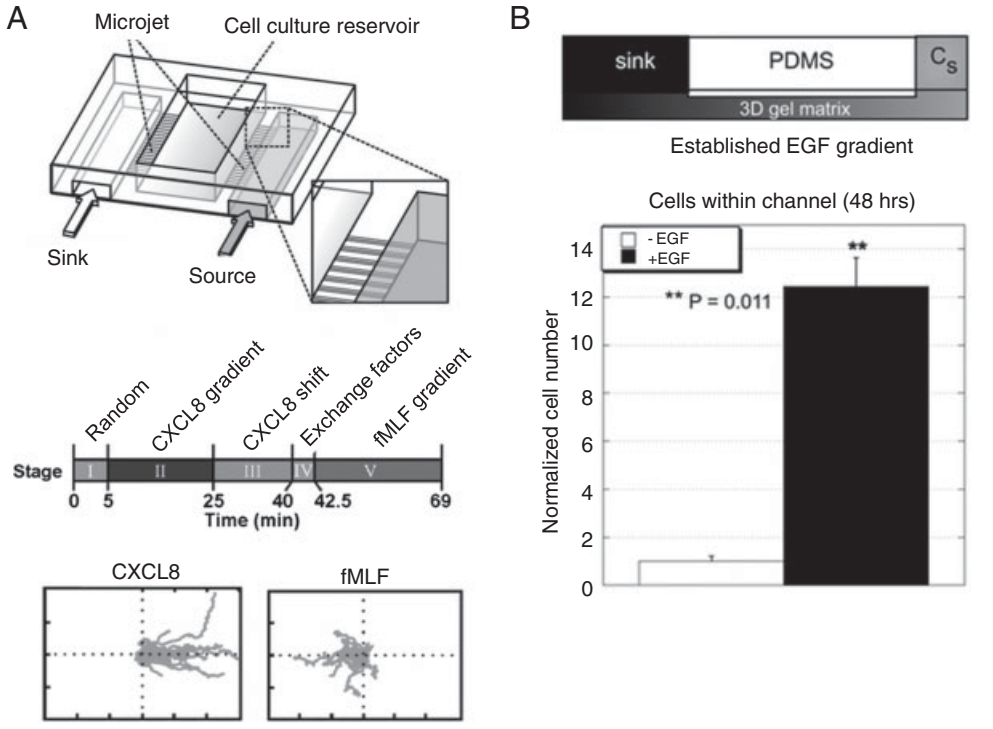

Figure 2. Microfluidic chemotaxis devices (A) neutrophil chemotaxis microject device containing a sink/source chamber and open cell culture reservoir that can generate chemoattractant gradients. Five stages are used for performing neutrophil desensitization and the migration tracking of the neutrophils exposed to dynamic gradients (reproduced by permission from The Royal Society of Chemistry [41]) and (B) cancer chemotaxis device that can create EGF gradients within 3-D gels and the quantitative analysis of the numbers of the cells in response to EGF gradients (reproduced by permission from The Royal Society of Chemistry [42]).

metastatic processes, such as intravasation and extravasation [44]. For the intravasation process, primary tumor cells enter the blood circulation [44]. The motility of invasive tumor cells exposed to extracellular molecular signals (*i.e.* chemokine) plays an important role in controlling metastasis and circulating cancer behavior [45, 46]. These circulating tumor cells also migrate from the blood vessel to the tissues during extravasation process [44].

Despite the development of animal models [44] and microscope techniques [46], the major limitation for studying cancer chemotaxis and metastasis is the inability to make an appropriate experimental model *in vitro* and the lack of tracking tumor cells in a real-time manner. To overcome these limitations, various microfabricated platforms have been previously developed [47–50]. For example, metastatic breast cancer cells have been used to study chemotaxis in response to the linear and nonlinear EGF gradients in a flow-based microfluidic device [47]. It was revealed that the metastatic breast cancer cells exposed to the nonlinear EGF gradients showed more directional movement as compared with linear gradients. Furthermore, a microfluidic gradient device has been used to study the interaction between the cancer chemotaxis and antibody against the EGF receptor [51]. The quantitative analysis showed that the EGF receptor played an important role in regulating the chemotaxis. It has been shown that the human breast cancer cells exposed to EGF gradients (0–50 ng/mL) were polarized toward higher concentration of EGF. In contrast, cancer cells treated with anti-EGF receptor were randomly polarized, suggesting that anti-EGF receptor inhibited chemotaxis. Therefore, the effect of anti-EGF receptor on human breast cancer cell motility has been observed in a gradient-generating microfluidic device.

In addition to flow-based microfluidic gradient devices on a 2D surface, a diffusion-based gradient platform in a well-defined 3-D microenvironment has been used to study the metastasis of invasive rat mammary adenocarcinoma cells (Fig. 2B) [42]. A diffusion-based stable EGF gradient was generated within a 3-D gel matrix of a bridge microchannel connected between sink and source microchannels. The invasive migratory behavior of the cells exposed to EGF gradients was analyzed by counting cell numbers in a bridge microchannel. A multi-step microfluidic device containing deformation and transmigration chambers has also been developed to study cancer metastasis [50]. Cancer cells were seeded into one microchannel and chemoattractant solution was added into the other microchannel in which endothelial cells were cultured. The chemoattractant gradient was generated within microbridge channels treated with Matrigel. This system can mimic the extravasation of primary tumor cells *in vivo*. Cancer cells exposed to the gradient of fetal bovine serum (FBS) were migrated through matrigel-coated microbridge channels. Furthermore, a gradient-generating microfluidic device containing two parallel perfusion and cell culture channels has been used to assess the invasion of breast cancer cells in a 3-D gel matrix [52]. It has been shown that the cells in response to EGF gradients formed long protrusion in a 3-D gel matrix, resulting in migration toward higher concentration of EGF. In contrast, the cells that were not stimulated by EGF gradients remained to be round. To study the effect of matrix metalloprotein (MMP) on cancer invasion in a 3-D gel matrix,

GM 6001, an MMP inhibitor, has also been used. It was revealed that MMP inhibitor restrained EGF-induced cancer invasion in a 3-D gel matrix, showing that both the EGF-induced cancer cell migration and the protrusion were significantly inhibited by an MMP inhibitor. Therefore, an MMP inhibitor could be a potentially powerful therapeutic candidate for treating cancer metastasis.

3.3 Bacteria growth and chemotaxis

Bacteria can swim by rotating their flagella in response to chemical gradients or signals [53, 54]. The flagellar switch, which plays an important role in controlling bacteria chemotaxis, is regulated by ion-derived rotary motors (*i.e.* motility protein A (MotA), motility protein B (MotB)) [53, 54]. The flagellar switch proteins (*i.e.* FliG, FliM, and FliN) enable the control of flagellar rotation and rotational direction, such as clockwise or counterclockwise [54]. Unfortunately, conventional assays for studying bacteria chemotaxis (*i.e.* swim plate, capillary assay) have the inability to quantify the migration in a temporal and spatial manner.

Microfluidic gradient devices have been previously used to investigate bacterial chemotaxis [18, 55–60]. For example, the migration of bacterial cells was analyzed in a flow-based microfluidic device containing three inlets and 22 outlets [18]. Gradients were generated in a 18-mm long main microchannel and each outlet port has different concentrations of chemoeffectors, such as L-aspartate, L-serine, and L-leucine. It demonstrated that L-leucine was attracted by the Tar receptor, whereas it was repelled by the Tsr receptor. A flow-based ''T''-shaped microchannel has been used to investigate the movement of chemotactic bacteria [59]. It was revealed that bacteria were moved in perpendicular to the direction of the fluidic flow. Furthermore, the serpentine-based microfluidic device containing flow-based diffusive mixing and cell culture area has been used to study the chemotaxis of *E. coli* exposed to the individual and competing linear gradients of signaling molecules [60]. Quantification data showed that *E. coli* was migrated toward a canonical attractant (*i.e.* L-aspartate) but away form repellent (*i.e.* Ni^{2+}). It was revealed that bacteria could migrate toward or away from cell–cell interaction signals, showing that the quorum-sensing molecule autoinducer-2 (AI-2) signal attracted to *E. coli*, but the stationary-phase signal indole repelled to *E. coli*. The diffusion-based gradient generator has also been used to study bacterial chemotaxis [56]. This device was consisted of three layers, such as a plastic of reagent reservoir, nitrocellulose membrane (0.45 μm pore size, 140 μm thickness) containing three microchannels, and glass substrate. The linear gradient of chemoattractant (*i.e.* L-aspartate) and chemorepellent (*i.e.* glycerol) molecules was generated by diffusion from nitrocellulose membrane. The quantitative analysis showed that wildtype *E. coli* strain RP437 was migrated toward L-aspartate and away from glycerol in a diffusion-based microfluidic device.

In addition to chemical gradients, oxygen gradient has been generated in a microfluidic device for controlling bacteria growth [61, 62]. The concentration of oxygen was generated by using PDMS-based two layers, such as flow and gas layer (Fig. 3) [61]. The serpentine microchannel enabled the generation of various oxygen concentrations in the top gas layer. Oxygen gas mixed in the top layer was diffused through a PDMS membrane (50 μm thickness). The growth of bacteria cultured in a flow channel was strongly affected by oxygen concentrations. Bacteria exposed to 12% oxygen concentration were more grown as compared with 0% oxygen concentration. It was revealed that the division rate of bacteria exposed to 12% oxygen concentration was approximately 5 times higher than 0% oxygen concentration. Similarly, the multiplexed oxygen concentration gradients have been developed by using two PDMS layers [62]. Different dissolved oxygen concentrations were generated by an oxygen–nitrogen mixing and were analyzed by using an oxygen-sensitive dye (*i.e.* platinum(II) octaethylporphine ketone (PtOEPK) dye) and light-emitting diode. It demonstrated that the cell density at 12 ppm dissolved oxygen concentration was much higher than 0 and 42 ppm dissolved oxygen concentrations after culturing for 8 days *in vitro*. Thus, the bacteria growth was significantly controlled by the gradient of oxygen concentrations.

3.4 Stem cell differentiation

Stem cell is a promising cell type for regenerative medicine and cell-based therapy, because it can differentiate into specific cell lineages [63–66]. Embryonic stem cells are derived from the blastocyst (*i.e.* inner cell mass), adult stem cells are obtained from the tissue-specific environment

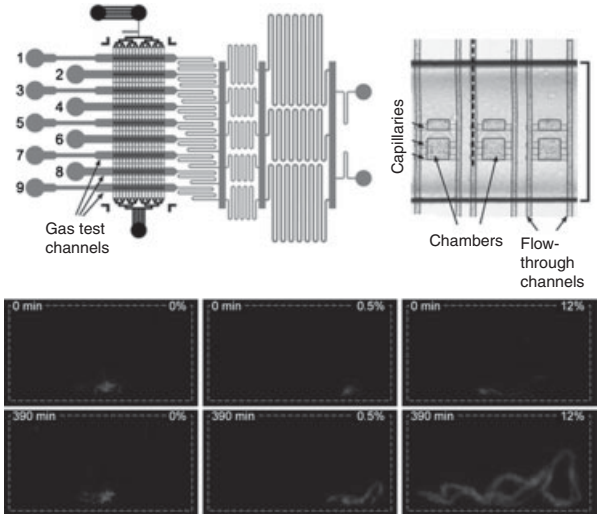

Figure 3. Bacteria growth in an oxygen gradient-generating microfluidic platform fabricated by a multi-layer soft lithography technique, showing *E. coli* colonies in response to different oxygen concentrations (0, 0.5, and 12%) (reproduced by permission from The Royal Society of Chemistry [61]).

(*i.e.* bone marrow, muscle), and induced pluripotent stem cells are derived from a human skin (*i.e.* fibroblast) [67]. In particular, induced pluripotent stem cells hold the unlimited self-renewal potential that is similar to the pluripotency of embryonic stem cells. Although induced pluripotent stem cells overcome the limitations (*i.e.* immune response, ethical problem) imposed by embryonic and adult stem cells, their efficiency is still low [67]. In addition, despite the potential of stem cells for treating degenerative diseases and human disorders, major challenges to prevent widespread use for clinical cell-based therapeutic applications are remained, such as the inability to control the growth and differentiation of stem cells in a homogeneous manner [63]. Unfortunately, the conventional culture methods have the inability to control the stem cell behavior in a well-defined microenvironment. To address these limitations, microfabricated gradient platforms have been recently developed to mimic the embryonic development as well as to understand the regulatory mechanism to direct embryonic and adult stem cell fate.

The microfabricated gradient platforms have the potential to regulate cell-soluble factor interaction. For instance, the growth and differentiation of human neural stem cells have been investigated in a flow-based microfluidic device (Fig. 4A) [21]. Neural stem cells can self-renew and differentiate into three cell types, such as neuron, astrocyte, and oligodendrocyte. The concentration gradients of growth factor mixtures containing EGF, fibroblast growth factor 2 (FGF2), and platelet-derived growth factor were stably generated in a microfluidic device as conventional assays have not previously been possible. The quantitative analysis showed that the growth of human neural stem cells

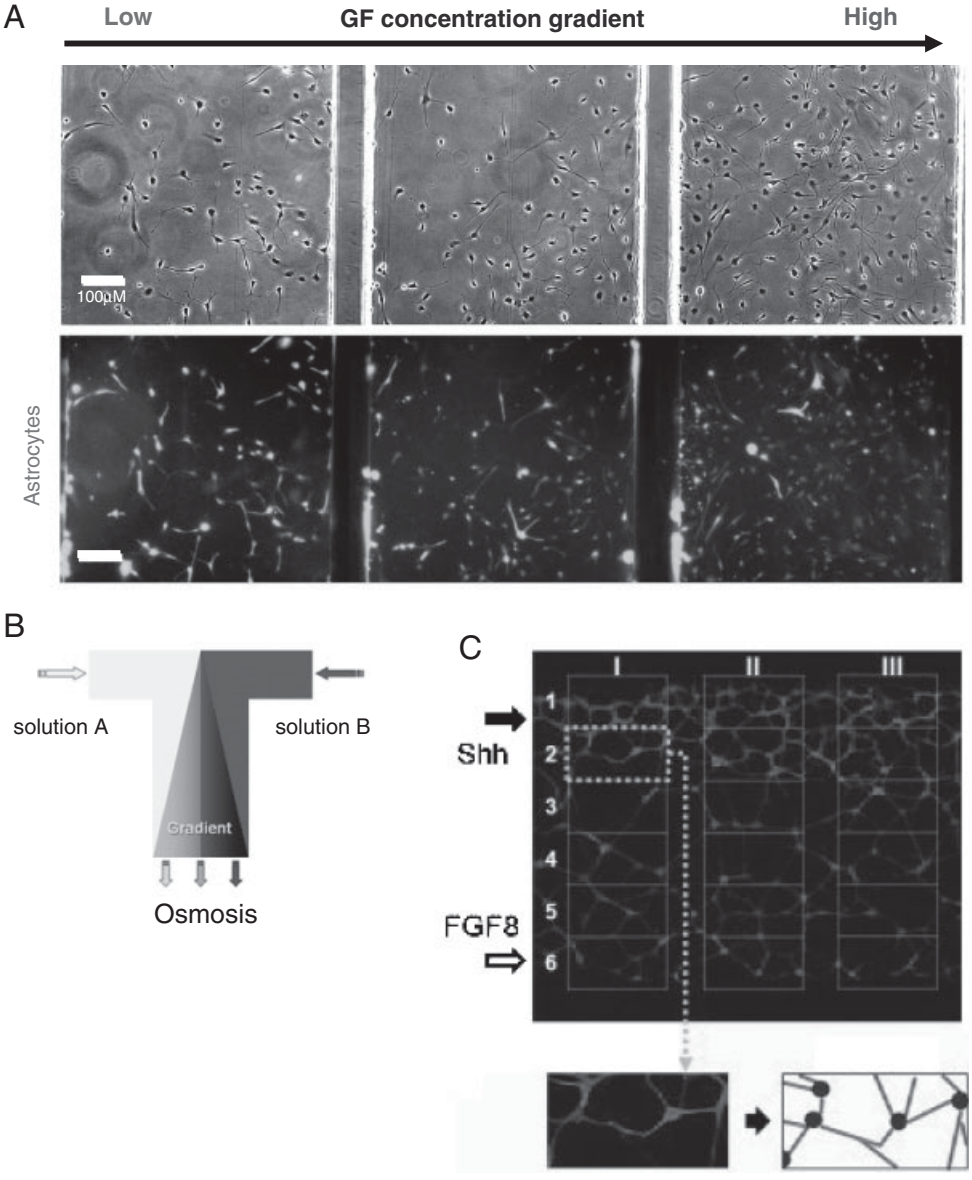

Figure 4. Stem cell differentiation in flow-based microfluidic devices. (A) The growth and differentiation of human neural stem cells exposed to stable growth factor (GF) gradients (reproduced by permission from The Royal Society of Chemistry [21]). (B) Osmotic pump-derived gradient assay for controlling the cellular behavior (reproduced by permission from The Royal Society of Chemistry [69]). (C) Fluorescent image of neural progenitor cell-derived neurons in an osmotic pump-based Shh/FGF8 gradient device. It shows different neuronal networks and neurite bundles in response to Shh/FGF8 gradients, confirmed by TuJ1 antibody immunostaining (reproduced by permission from AlphaMed Press [70]).

was directly proportional to growth factor concentrations, whereas their differentiation into astrocyte was inversely proportional to growth factor concentrations. To regulate the growth and death of mouse neural stem cells, a flow-based hybrid microfluidic-vacuum device has been previously developed [68]. Unlike previously developed microfluidic culture devices, this hybrid microfluidic-vacuum platform containing a fluidic microchannel and vacuum network can directly apply to the cells cultured on a cell culture dish without the step of cell seeding into a microfluidic device through cell inlet ports. The vacuum network enabled the reversible bonding between a microfluidic device and a cell culture dish. The real-time live/dead assay containing a cell-impermeant propidium iodide showed that mouse neural stem cells exposed to the gradients of oxidative stress (*i.e.* 50 mM of hydrogen peroxide) induced the rapid cell death.

The attachment and proliferation of human mesenchymal stem cells (MSCs) have been investigated by using an osmotic pump-based microfluidic device (Fig. 4B) [69]. The osmotic pump containing a glass tube and cellulose membrane within a PDMS chamber enabled the control of flow rate and fetal bovine serum gradient profiles. The immunocytochemistry results showed that cell attachment and proliferation were increased with increasing concentrations of fetal bovine serum gradients. The osmotic pump-based microfluidic device has been recently used to study the proliferation and differentiation of neural progenitor cells derived from human embryonic stem cells (Fig. 4C) [70]. This device mimicked to generate sonic hedgehog (Shh), FGF8, and bone morphogenetic protein 4 (BMP4) gradients that could be created during early brain development. The quantitative analysis of overlapping exogenous cytokine gradients (Shh/FGF8 or Shh/BMP4) showed that TuJ1-positive neurons were more highly expressed in Shh/FGF8 gradients as compared with Shh/BMP4 gradients. This approach could be a potentially useful for studying the effects of agonist (*i.e.* Shh) and antagonist (*i.e.* BMP4) on the neuronal differentiation derived from human embryonic stem cells.

The biomechanical force (*i.e.* shear stress) plays an important role in regulating the proliferation and differentiation of embryonic and adult stem cells [71–75]. For example, the effect of shear stress on mouse embryonic stem cell-derived hematopoietic differentiation has been studied to demonstrate whether the vascular wall shear stress acts as a hematopoietic potential [71]. Mouse embryonic stem cell-derived embryoid bodies (EBs) were created by using a hanging drop method and their cell monolayers were subsequently exposed to shear stress for 48 h. The quantitative analysis demonstrated that the cells exposed to wall shear stress showed the upregulation of the hematopoietic markers, such as *Runx1*, *Myb*, and *Klf2*, indicating biomechanical stimulus (*i.e.* shear stress)-mediated hematopoietic potential. The rotary orbital-based hydrodynamic force has also modulated the mouse embryonic stem cell differentiation [72]. The EB size was increased by decreasing rotary orbital speed, because slow rotational speeds generated low shear stress and uniform hydrodynamic conditions. Temporal gene expression analysis showed that the EB differentiation was regulated by rotary orbital speed, indicating that Gata-4 (mesoderm/endoderm marker) was highly expressed at a low rotary orbital speed (25 rpm), whereas nestin (ectoderm marker) expression was significantly increased by increasing rotary orbital speed (~55 rpm). The shear stress generated in rotary orbital culture system enabled the control of the EB size and differentiation. In case of adult stem cells, MSCs can be exposed to blood fluid shear stress after transplantation [73]. It has been shown that the shear stress generated inside a conventional flow chamber has induced proteome change of human MSCs, showing that it increased Annexin A2 protein expression that could affect the function of MSCs. However, previous approaches did not use microfluidic device that could generate various shear stress profiles. To our knowledge, a few approaches have been reported to investigate the effect of shear stress on stem cell differentiation in microfluidic platforms. For example, the effect of shear stress on bone marrow stromal cell behavior has been studied by using a poly(methyl methacrylate) (PMMA)-based radial-flow microchamber [74]. The cells were exposed to shear stress in a PMMA microchamber. It has been shown that the proliferation of bone marrow stromal cells was not affected by shear stress, whereas their osteoblastic maturation (prostaglandin signaling in bone marrow stromal cell differentiation) was significantly dependent on applied shearing flow. It was revealed that the osteocalcin protein of the cells exposed to shear stress was increased as compared with static controls. Thus, shearing flow is a powerful means to develop osteoblastic maturation and stimulate bone marrow stromal cell differentiation. Another approach is to use the logarithmically perfused microfluidic array system that could create logarithmic concentration gradients in a well-defined microenvironment [75]. Mouse embryonic stem cells exposed to higher shear stresses were self-aggregated to become larger colonies in a perfused microfluidic array system. A number of colonies were decreased with increasing flow rates. It was revealed that flow rates enabled the control of colony size and number in mouse embryonic stem cells, because the nutrient delivery and waste removal could be increased at higher flow rate. Therefore, shear stress generated in a microfluidic device is a potentially powerful approach to investigate the effect of shear stress on stem cell differentiation.

A diffusion-based gradient device has also been used to culture human embryonic stem cells [76]. A device developed by the multi-layer soft lithography technique was consisted of aperture template (top layer), microwell reservoir embedding the porous membrane with 0.2 μm pore diameter (middle layer), and assay microchannel (bottom layer) that could generate molecular gradients. A small droplet with cell suspension on an aperture template enabled the generation of the spatio-temporal patterning in an assay microchannel through the microwell reservoir.

Thus, human embryonic stem cells were patterned on a mouse embryonic fibroblast feeder layer. Furthermore, murine mammary gland epithelial cells exposed to the gradient of the exogenous factor were patterned on an assay microchannel. Therefore, these microfluidic gradient platforms could be potentially useful tools for controlling embryonic development and directing stem cell fate.

3.5 Axon guidance

Neurons are of great interest in controlling the traumatic injury of spinal cord and neurodegenerative diseases (*i.e.* Alzheimer disease) [77]. Axonal regeneration enables the treatment of nerve injury in the central nervous system [78]. Thus, the understanding of behavior and mechanism of axonal guidance is important for studying the axonal regeneration. Campenot chamber has been previously used for regulating the neurite development of sympathetic neurons *in vitro* [79]. Campenot chamber is consisted of three-chamber culture system and a Teflon divider in a cell culture dish. The growth of neurites was strongly regulated by nerve growth factor in a Campenot chamber.

Recently, a microfluidic culture platform that can completely isolate axons and somas in a controlled manner has been developed for studying axonal injury and regeneration [80]. The immunocytochemistry and reverse transcription polymerase chain reaction analysis showed that axotomy induced the transcription of lesioned somas and neurotrophins improved axonal regeneration. Although this device enabled the isolation of axons to screen the biomolecules that played an important role in controlling axonal regeneration, it did not study the gradient-based axon guidance or neurite outgrowth. A flow-based microfluidic device has been previously used to control axon guidance of neurons [81]. Rat hippocampal neurons were cultured on substrate-bound gradients of laminin. It was revealed that axons were oriented toward higher density of laminin in a microfluidic device. To create substrate-bound gradients of axon guidance proteins on a 2D surface, the surface patterning technique (*i.e.* microcontact printing) has been used in a microfluidic channel. For example, the stepwise gradients of the substrate-bound ephrinA5 molecule have been generated to regulate the behavior of growth cones of chick retinal ganglion cells [82]. The quantitative analysis represented that the axons exposed to ephrinA5 gradients were extended. However, the outgrowth of growth cones was stopped at a certain concentration, showing that the biomolecule gradients played an important role in controlling the behavior of axonal guidance and growth cone outgrowth.

The mechanical stiffness enables the control of the cellular fate and function [83]. Cell migration can be controlled by mechanical stiffness, called ''durotaxis'' [84]. To study the effect of mechanical stiffness on neuronal function, an ''H''-shaped microfluidic device has been used to control neurite outgrowth of the chick dorsal root ganglia in a 3-D gel [85]. The gradients of genipin that could control the mechanical stiffness were generated by using a source and sink microchannel network filling in collagen type I. The linear gradients of genipin-induced crosslinking created at the bridge channel of an ''H''-shaped microfluidic device were evaluated by measuring the fluorescent intensity. The quantitative analysis showed that the average neurite length of chick dorsal root ganglia was controlled by genipin gradients.

3.6 Endothelial cell migration

Directed cell migration in response to chemoattractant gradients is of great interest in controlling embryonic blood vessel formation and angiogenic sprouts [86]. In particular, vascular endothelial growth factor (VEGF) plays a significant role in regulating hierarchical vascular formation, tubular sprouting, and fusion [87]. Endothelial cells cultured within a blood vessel can be exposed to the gradients of the secreted signaling proteins, resulting in forming new blood vessels and promoting angiogenesis. Despite their potential, the response of endothelial cells in response to VEGF gradients is not clearly understood [86].

Microfluidic-based gradient platforms have been previously used to control endothelial cell migration and angiogenesis. For example, a flow-based microfluidic-vacuum device has been used to study endothelial cell migration in response to growth factors [86]. It demonstrated that endothelial cell migration was strongly affected by gradient steepness and VEGF-A types, such as VEGF165 and VEGFA121. In addition to the endothelial cell migration in a microfluidic device, a hydrogel gradient has been generated to study endothelial cell attachment [88]. The linear gradient of poly(ethylene glycol) (PEG) conjugated arginine–glycine–aspartic acid (RGDS) peptides was created in a serpentine-based microfluidic device. It was revealed that the endothelial cells exposed to higher concentration of RGDS were highly attached in a microfluidic channel. Furthermore, a convection flow-based microfluidic device has been used to generate long-range material gradient and endothelial cell gradient [89]. To investigate cell-biomaterial interaction, the PEG hydrogel gradient and cross-gradient of composite materials (*i.e.* hyaluronic acid, gelatin) was laterally generated in a simple microchannel. Interestingly, endothelial cell gradient was created by using high-speed fluidic flow, showing different cell density in response to gradient profiles in a microchannel.

Microfluidic devices have been used to study capillary formation and angiogenesis in a 3-D microenvironment [90, 91]. For example, a diffusion-based microfluidic gradient platform containing 3-D collagen scaffolds has been used to study cell migration, capillary formation of human adult dermal microvascular endothelial cells, and sprouting angiogenesis [90]. Time-lapse cell analysis showed the behavior of endothelial cell sprouting to form capillary

(*i.e.* lumen-like structure) and migration mechanism of endothelial cells encapsulated within collagen gels. The capillary growth and endothelial cell migration have also been investigated in a 3-D matrix microchannel, where cancer and smooth muscle cells or cancer and HMVECs were co-cultured (Fig. 5) [91]. The quantitative analysis showed that the molecules secreted from cancer cells attracted endothelial cells, resulting in capillary growth (Fig. 5A). Cancer cells seeded at high density more attracted the HMVECs into a 3-D collagen scaffold as compared with low-density cancer cells, because the secreted molecules were more obtained from high-density cell population. The migration speed of U87MG cancer cells was faster as compared with MTLn3 cancer cells (Fig. 5B). Furthermore, the interaction between endothelial cells and vascular smooth muscle cells was investigated in a microfluidic device (Fig. 5C). It was revealed that smooth muscle cells (10T 1/2) suppressed endothelial cell activity, showing that endothelial cells migrated to the control side. Therefore, a microfluidic device that generate molecular gradients in a 3-D scaffold could be a useful tool to study endothelial cell migration and angiogenesis.

3.7 Yeast mating

Yeast (*i.e. Saccharomyces cerevisiae*) mating is the fusion of α-cell and **a**-cell, showing that α-cell secretes α-factor that can bind to **a**-cell receptor (*i.e.* Ste2) [92]. The G protein-coupled receptors play an important role in controlling yeast mating, budding, and polarization. In particular, the yeast is asymmetrically grown during the budding and mating process, resulting in yeast polarization [93]. A spatial gradient sensing of the mating pheromone α-factor has been recently investigated in a flow-based ''Y''-shaped microfluidic device (Fig. 6A) [94]. The yeast cells were sensitively responded by α-factor concentration gradients. In particular, cell morphologies were strongly affected by α-factor concentrations, indicating that the yeast cells exposed to lower concentrations became cluster, but thin

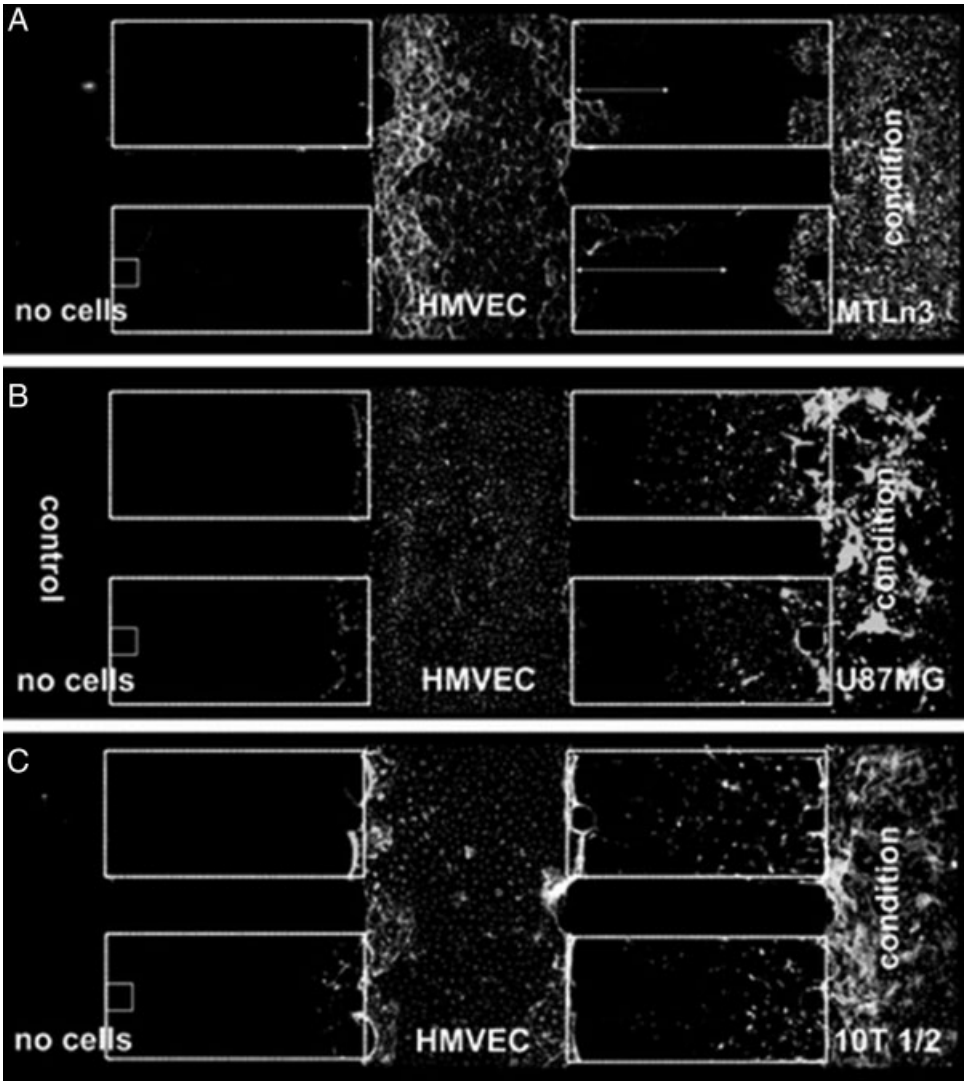

Figure 5. Cell migration in a microfluidic collagen scaffold gradient device containing various co-culture systems. (A) Endothelial cell (HMVEC) migration in the co-culture with cancer cell (MTLn3). (B) Co-culture of HMVEC and cancer cell (U87MG). (C) Co-culture of HMVEC and vascular smooth muscle cell (10T 1/2), showing HMVEC migration into the control side (reproduced by permission from The Royal Society of Chemistry [91]).

shmoo shape was found in higher concentrations. The quantitative analysis showed that the gradient slopes and concentration profiles played a significant role in regulating the direction and polarization of yeast cells. This gradient-generating microfluidic device has the potential to study spatial gradient sensing of yeast cells, mechanism of yeast polarization, and their G-protein signaling in a controlled manner. A diffusion-based microfluidic device has also been used to study gradient sensing in yeast (Fig. 6B) [95]. The pheromone gradients were generated in a bridge test chamber connected the sink and source microchannel and fluidic flow was controlled by the microvalves. It was revealed that mitogen-activated protein kinase enabled the control of a transcription factor, Ste12, of pheromone in a microfluidic device. This approach could be a potentially useful for regulating the mating pathway of yeast cells in a temporal and spatial manner.

3.8 Cytotoxicity

Environmental toxicants play a critical role in controlling human health [96]. Cadmium, one of environmental toxicants, has been widely used in a fertilizer and battery, resulting in increasing the chance to the exposure of cadmium [97]. To study the effect of cadmium on the cell viability, cadmium-induced cytotoxicity has been investigated in a flow-based gradient-generating microfluidic device containing a diffusion diluter and cell culture microchannel [98]. The cytotoxic effect of cadmium on fibroblast cells was analyzed by a live/dead assay and apoptotic assay. It demonstrated that the percentage of apoptotic cells was proportional to cadmium concentrations. It was also revealed that cadmium-induced apoptosis was caused by the oxidative stress and cytoskeleton disorganization. To study anti-cancer drug-induced apoptosis in a high-throughput manner, an integrated microfluidic platform containing multiple flow-based liner gradient generators has also been developed [99]. In this high content screening platform, human liver carcinoma (HepG2) cells were used to investigate concentration-dependent toxicity. It was revealed that deoxyribonucleic acid of the cells exposed to anti-cancer drugs was damaged and their ribonucleic acid synthesis was restrained, resulting in drug-induced apoptosis. Therefore, the high content screening-based microfluidic platform that could analyze the plasma membrane permeability and mitochondrial transmembrane potential enabled the screening of the anti-cancer drugs in a rapid and parallel manner. Furthermore, the flow-based long-range concentration gradient in a portable microfluidic device has been developed to study the cytotoxicity of cardiac muscle cells [28]. The concentration gradient was created by evaporation and surface tension in a 5-cm-long microchannel. The viability of cells exposed to gradients of cardiac toxin (*i.e.* alpha-cypermethrin) was inversely proportional to concentrations of alpha-cypermethrin. In addition to concentration gradients on a 2D surface, microfluidic-based hydrogel gradient has been developed in a 3-D microenvironment [100]. The hepatocytes and self-assembling peptide hydrogel (*i.e.* Puramatrix) were patterned in the middle of

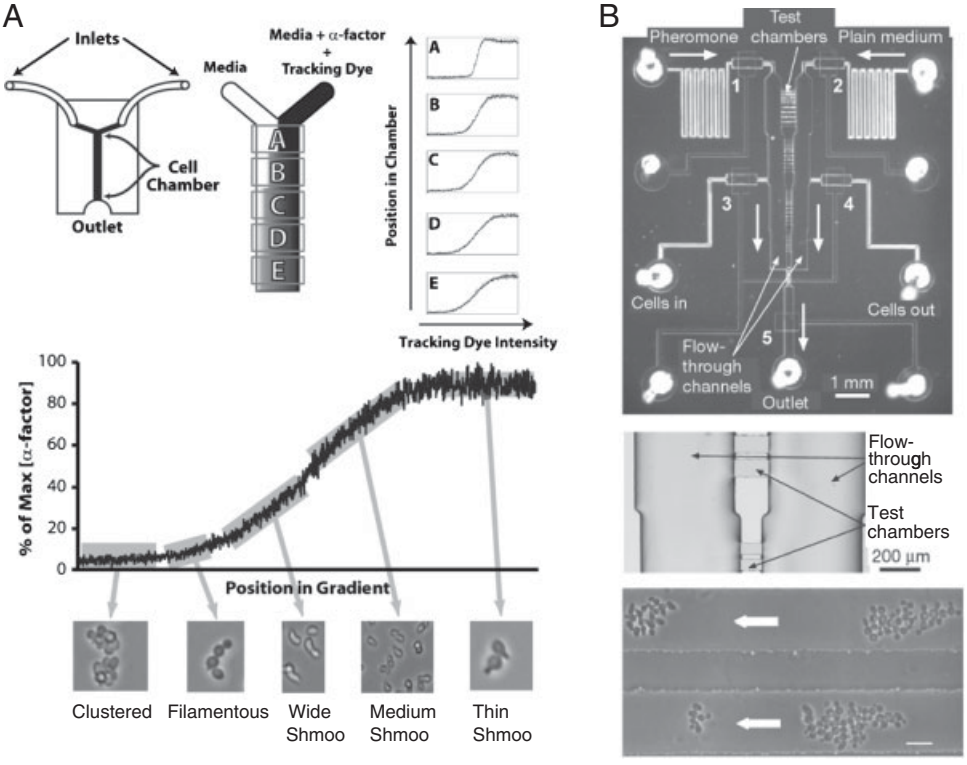

Figure 6. Yeast-mating response in a pheromone gradient-generating microfluidic device. (A) Various cell morphologies in a *Y*-shape device that can generate α-factor gradients (reproduced by permission from The Public Library of Science [94]). (B) Pheromone gradient sensing of yeast cells cultured in a microfluidic device containing a bridge test chamber connected with two flow-through channels (reproduced by permission from Macmillan Publishers Ltd. [95]).

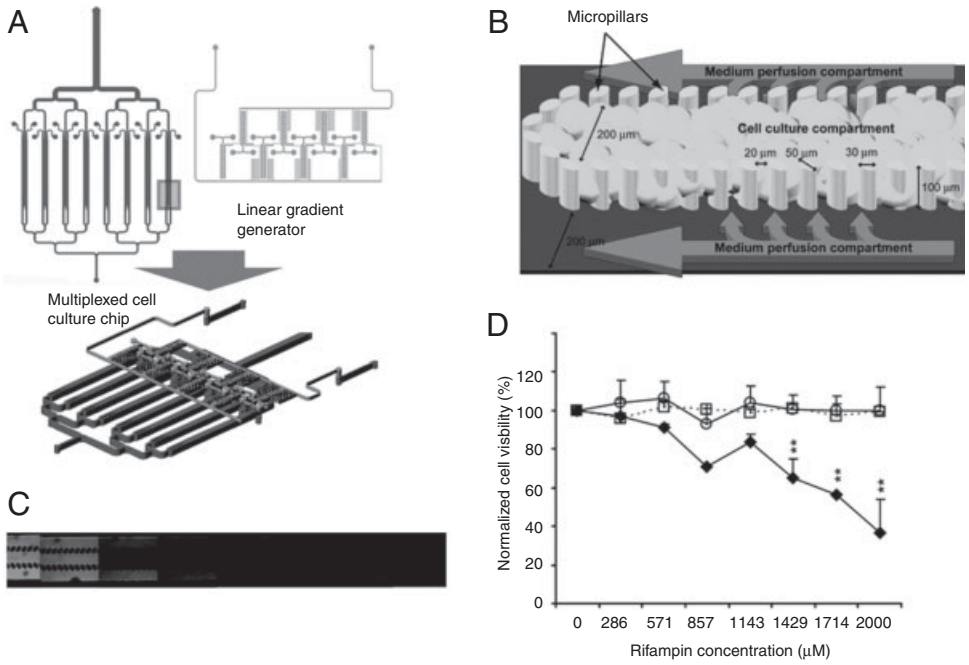

Figure 7. The 3-D microfluidic device for drug toxicity testing. (A) A design of a multiplexed microfluidic device that can generate linear gradients. (B) A micropillar array and two compartments for cell culture and medium perfusion. (C) Fluorescent image to confirm linear gradients. (D) Hepatotoxicity analysis from 3-D microfluidic device and well-plates (♦: 3-D microfluidic device, ○: multi-well plate, and □: dimethyl sulfoxide (DMSO) control) (reproduced by permission from The Royal Society of Chemistry [101]).

three inlet microchannels. The linear concentration gradients of a toxicant (*i.e.* Triton X-100) were established in a cell-laden 3-D peptide scaffold. It was revealed that the number of dead cells was increased with increasing toxicant concentrations. A microfluidic 3-D gradient-generating multiplexed device has also been developed for studying drug hepatotoxicity (Fig. 7) [101]. A multiplexed microchannel that was consisted of cell culture compartment and medium perfusion compartment enabled the screening of dose-dependent multiple drug responses (Fig. 7A–B). The positively charged methylated collagen and negatively charged HEMA-MMA-MAA terpolymer were used for creating 3-D matrix in a microchannel. Hepatotoxicity analysis obtained from five model hepatotoxic drugs (*i.e.* acetaminophen, diclofenac, quinidine, rifampin, and ketoconazole) showed that drug-based hepatotoxicity was affected by its metabolism. It was also revealed that the drug-mediated hepatotoxicity was more sensitive in a 3-D hepatocyte device as compared with a multi-well plate (Fig. 7D). Furthermore, a cell-laden microfluidic agarose gel device has been developed by using a soft lithographic technique [102]. Murine hepatocytes were encapsulated within a 3-D agarose microchannel that could mimic microvascularized structures *in vivo*. Cell viability was analyzed as a function of the medium diffusion from microchannel surface, showing that the viability was significantly decreased at the 550–1050 μm distance from the microchannel surface after culturing for 3 days *in vitro*.

4 Conclusion and future direction

The microfluidic platform that can generate chemical, mechanical, material, and oxygen gradients is an enabling method to regulate cell–extracellular microenvironment interaction for various biological applications, such as chemotaxis, embryogenesis, and axon guidance. As compared with conventional gradient assays, the microfluidic-based gradient devices enable the control of the fluidic flow and diffusion profiles in a temporal and spatial manner. In this paper, we review the recent development of various flow- and diffusion-based microfluidic gradient platforms on a 2-D surface and 3-D hydrogel microenvironment and also highlight their biological applications (Table 1). Despite the advanced microscale technologies, there are still many limitations that prevent the widespread use as a biological tool, such as the complicated microfabrication process. To overcome these limitations, engineers and biologists have to be collaborated each other. A close collaboration between two research groups enables the generation of various potential engineering culture platforms, such as the integrated culture device that can control chemical, material, and oxygen gradients at the same time or biocompatible hydrogel-based microfluidic device that can directly transplant into animals *in vivo* for high-throughput drug screening. To better control cellular behavior and real-time molecular imaging, top-down approach (*i.e.* microfluidic device) needs to be merged with bottom-up approach (*i.e.* nanopatterning, nanomaterial-based peptide scaffold, and nanoparticle). Therefore, this approach could be potentially useful for cell biologists to understand the mechanism of the gradient-sensing and its underlying cell biology.

This paper was supported by Basic Science Research Program through the National Research Foundation of Korea (NRF) funded by the Ministry of Education, Science and Technology (Grant Number R11-2008-044-01002-0) and Korea

Industrial Technology Foundation (KOTEF) through the Human Resource Training Project for Strategic Technology.

The authors have declared no conflict of interest.

5 References

[1] Gurdon, J., Bourillot, P., *Nature* 2001, *413*, 797–803.

[2] Keenan, T. M., Folch, A., *Lab Chip* 2008, *8*, 34–57.

[3] Paguirigan, A. L., Beebe, D. J., *Bioessays* 2008, *30*, 811–821.

[4] Rogulja, D., Irvine, K. D., *Cell* 2005, *123*, 449–461.

[5] Baggiolini, M., Dewald, B., Moser, B., *Annu. Rev. Immunol.* 1997, *15*, 675–705.

[6] Janetopoulos, C., Ma, L., Devreotes, P. N., Iglesias, P. A., *Proc. Natl. Acad. Sci. USA* 2004, *101*, 8951–8956.

[7] Foxman, E. F., Campbell, J. J., Butcher, E. C., *J. Cell Biol.* 1997, *139*, 1349–1360.

[8] Boyden, S., *J. Exp. Med.* 1962, *115*, 453–466.

[9] Zigmond, S. H., *J. Cell Biol.* 1977, *75*, 606–616.

[10] Zicha, D., Dunn, G., Jones, G., *Methods Mol. Biol.* 1991, *75*, 449–457.

[11] Gundersen, R. W., Barrett, J. N., *Science* 1979, *206*, 1079–1080.

[12] Zheng, J. Q., Felder, M., Connor, J. A., Poo, M. M., *Nature* 1994, *368*, 140–144.

[13] Lohof, A. M., Quillan, M., Dan, Y., Poo, M. M., *J. Neurosci.* 1992, *12*, 1253–1261.

[14] Segall, J. E., *Proc. Natl. Acad. Sci. USA* 1993, *90*, 8332–8336.

[15] Jeon, N. L., Baskaran, H., Dertinger, S. K. W., Whitesides, G. M., Van de Water, L., Toner, M., *Nat. Biotechnol.* 2002, *20*, 826–830.

[16] Abhyankar, V. V., Lokuta, M. A., Huttenlocher, A., Beebe, D. J., *Lab Chip* 2006, *6*, 389–393.

[17] Irimia, D., Geba, D. A., Toner, M., *Anal. Chem.* 2006, *78*, 3472–3477.

[18] Mao, H. B., Cremer, P. S., Manson, M. D., *Proc. Natl. Acad. Sci. USA* 2003, *100*, 5449–5454.

[19] Wu, H. K., Huang, B., Zare, R. N., *J. Am. Chem. Soc.* 2006, *128*, 4194–4195.

[20] Tourovskaia, A., Li, N. Z., Folch, A., *Biophys. J.* 2008, *95*, 3009–3016.

[21] Chung, B. G., Flanagan, L. A., Rhee, S. W., Schwartz, P. H., Lee, A. P., Monuki, E. S., Jeon, N. L., *Lab Chip* 2005, *5*, 401–406.

[22] Beebe, D. J., Mensing, G. A., Walker, G. M., *Annu. Rev. Biomed. Eng.* 2002, *4*, 261–286.

[23] Whitesides, G. M., *Nature* 2006, *442*, 368–373.

[24] Weibel, D. B., Whitesides, G. M., *Curr. Opin. Chem. Biol.* 2006, *10*, 584–591.

[25] Whitesides, G. M., Ostuni, E., Takayama, S., Jiang, X., Ingber, D. E., *Annu. Rev. Biomed. Eng.* 2001, *3*, 335–373.

[26] Jeon, N. L., Dertinger, S. K. W., Chiu, D. T., Choi, I. S., Stroock, A. D., Whitesides, G. M., *Langmuir* 2000, *16*, 8311–8316.

[27] Dertinger, S. K. W., Chiu, D. T., Jeon, N. L., Whitesides, G. M., *Anal. Chem.* 2001, *73*, 1240–1246.

[28] Du,Y., Shim,J., Vidula,M., Hancock,M. J., Lo,E., Chung,B. G., Borenstein,J. T., Khabiry,M., Cropek, D. M., Khademhosseini,A., *Lab Chip* 2009, *9*, 761–767.

[29] Walker, G. M., Beebe, D. J., *Lab Chip* 2002, *2*, 131–134.

[30] Meyvantsson, I., Warrick, J. W., Hayes, S., Skoien, A., Beebe, D. J., *Lab Chip* 2008, *8*, 717–724.

[31] Cooksey, G. A., Sip, C. G., Folch, A., *Lab Chip* 2009, *9*, 417–426.

[32] Fosser, K. A., Nuzzo, R. G., *Anal. Chem.* 2003, *75*, 5775–5782.

[33] Chung, B. G., Lin, F., Jeon, N. L., *Lab Chip* 2006, *6*, 764–768.

[34] Kubes, P., *Semin. Immunol.* 2002, *14*, 65–72.

[35] Harvath, L., *EXS* 1991, *59*, 35–52.

[36] Kay, R. R., Langridge, P., Traynor, D., Hoeller, O., *Nat. Rev. Mol. Cell Biol.* 2008, *9*, 455–463.

[37] Lin, F., Nguyen, C. M. C., Wang, S. J., Saadi, W., Gross, S. P., Jeon, N. L., *Biochem. Biophys. Res. Commun.* 2004, *319*, 576–581.

[38] Lin, F., Nguyen, C. M. C., Wang, S. J., Saadi, W., Gross, S. P., Jeon, N. L., *Ann. Biomed. Eng.* 2005, *33*, 475–482.

[39] Irimia, D., Liu, S. Y., Tharp, W. G., Samadani, A., Toner, M., Poznansky, M. C., *Lab Chip* 2006, *6*, 191–198.

[40] Irimia, D., Balazsi, G., Agrawal, N., Toner, M., *Biophys. J.* 2009, *96*, 3897–3916.

[41] Keenan, T. M., Frevert, C. W., Wu, A., Wong, V., Folch, A., *Lab Chip* 2010, *10*, 116–122.

[42] Abhyankar, V. V., Toepke, M. W., Cortesio, C. L., Lokuta, M. A., Huttenlocher, A., Beebe, D. J., *Lab Chip* 2008, *8*, 1507–1515.

[43] Frevert, C. W., Boggy, G., Keenan, T. M., Folch, A., *Lab Chip* 2006, *6*, 849–856.

[44] Chambers, A. F., Groom, A. C., MacDonald, I. C., *Nat. Rev. Cancer* 2002, *2*, 563–572.

[45] Wells, A., *Adv. Cancer Res.* 2000, *78*, 31–101.

[46] Condeelis, J., Segall, J. E., *Nat. Rev. Cancer* 2003, *3*, 921–930.

[47] Wang, S. J., Saadi, W., Lin, F., Nguyen, C. M. C., Jeon, N. L., *Exp. Cell Res.* 2004, *300*, 180–189.

[48] Saadi, W., Wang, S. J., Lin, F., Jeon, N. L., *Faseb J.* 2005, *19*, A1505–A1505.

[49] Mosadegh, B., Saadi, W., Wang, S. J., Jeon, N. L., *Biotechnol. Bioeng.* 2008, *100*, 1205–1213.

[50] Chaw, K. C., Manimaran, M., Tay, E. H., Swaminathan, S., *Lab Chip* 2007, *7*, 1041–1047.

[51] Saadi, W., Wang, S. J., Lin, F., Jeon, N. L., *Biomed. Microdevices* 2006, *8*, 109–118.

[52] Liu, T., Li, C., Li, H., Zeng, S., Qin, J., Lin, B., *Electrophoresis* 2009, *30*, 4285–4291.

[53] Segall, J. E., Manson, M. D., Berg, H. C., *Nature* 1982, *296*, 855–857.

[54] Eisenbach, M., Caplan, S. R., *Curr. Biol.* 1998, *8*, R444–R446.

[55] Mao, H. B., VanWay, S., Manson, M., Cremer, P., *Biophys. J.* 2003, *84*, 521a–521a.

[56] Diao, J. P., Young, L., Kim, S., Fogarty, E. A., Heilman, S. M., Zhou, P., Shuler, M. L., Wu, M., DeLisa, M. P., *Lab Chip* 2006, *6*, 381–388.

[57] Kim, M. J., Breuer, K. S., *Anal. Chem.* 2007, *79*, 955–959.

[58] Nam, S. W., Van Noort, D., Yang, Y., Kim, S. H., Park, S., *Biochip J.* 2007, *1*, 111–116.

[59] Lanning, L. M., Ford, R. M., Long, T., *Biotechnol. Bioeng.* 2008, *100*, 653–663.

[60] Englert, D. L., Manson, M. D., Jayaraman, A., *Appl. Environ. Microb.* 2009, *75*, 4557–4564.

[61] Polinkovsky, M., Gutierrez, E., Levchenko, A., Groisman, A., *Lab Chip* 2009, *9*, 1073–1084.

[62] Lam, R. H., Kim, M. C., Thorsen, T., *Anal. Chem.* 2009, *81*, 5918–5924.

[63] Vazin, T., Schaffer, D. V., *Trends Biotechnol.* 2010, *28*, 117–124.

[64] Bhattacharya, B., Puri, S., Puri, R. K., *Curr. Stem Cell Res. Ther.* 2009, *4*, 98–106.

[65] Wobus, A. M., Boheler, K. R., *Physiol. Rev.* 2005, *85*, 635–678.

[66] Azarin, S. M., Palecek, S. P., *Biochem. Eng. J.* 2010, *48*, 378.

[67] Lutolf, M. P., Gilbert, P. M., Blau, H. M., *Nature* 2009, *462*, 433–441.

[68] Chung, B. G., Park, J. W., Hu, J. S., Huang, C., Monuki, E. S., Jeon, N. L., *BMC Biotechnol* 2007, *7*, 60.

[69] Park, J. Y., Hwang, C. M., Lee, S. H., Lee, S. H., *Lab Chip* 2007, *7*, 1673–1680.

[70] Park, J. Y., Kim, S. K., Woo, D. H., Lee, E. J., Kim, J. H., Lee, S. H., *Stem Cells* 2009, *27*, 2646–2654.

[71] Adamo, L., Naveiras, O., Wenzel, P. L., McKinney-Freeman, S., Mack, P. J., Gracia-Sancho, J., Suchy-Dicey, A., Yoshimoto, M., Lensch, M. W., Yoder, M. C., Garcia-Cardena, G., Daley, G. Q., *Nature* 2009, *459*, 1131–1135.

[72] Sargent, C. Y., Berguig, G. Y., Kinney, M. A., Hiatt, L. A., Carpenedo, R. L., Berson, R. E., McDevitt, T. C., *Biotechnol. Bioeng.* 2010, *105*, 611–626.

[73] Yi, W., Sun, Y., Wei, X., Gu, C., Dong, X., Kang, X., Guo, S., Dou, K., *Mol. Cell Biochem.* 2010, DOI 10.1007/s11010-010-0432-7.

[74] Kreke, M. R., Goldstein, A. S., *Tissue Eng.* 2004, *10*, 780–788.

[75] Kim, L., Vahey, M. D., Lee, H. Y., Voldman, J., *Lab Chip* 2006, *6*, 394–406.

[76] Abhyankar, V. V., Beebe, D. J., *Anal. Chem.* 2007, *79*, 4066–4073.

[77] McKerracher, L., *Neurobiol. Dis.* 2001, *8*, 11–18.

[78] Grados-Munro, E. M., Fournier, A. E., *J. Neurosci. Res.* 2003, *74*, 479–485.

[79] Campenot, R. B., *Proc. Natl. Acad. Sci. USA* 1977, *74*, 4516–4519.

[80] Taylor, A. M., Blurton-Jones, M., Rhee, S. W., Cribbs, D. H., Cotman, C. W., Jeon, N. L., *Nat. Methods* 2005, *2*, 599–605.

[81] Dertinger, S. K. W., Jiang, X. Y., Li, Z. Y., Murthy, V. N., Whitesides, G. M., *Proc. Natl. Acad. Sci. USA* 2002, *99*, 12542–12547.

[82] Lang, S., von Philipsborn, A. C., Bernard, A., Bonhoeffer, F., Bastmeyer, M., *Anal. Bioanal. Chem.* 2008, *390*, 809–816.

[83] Engler, A. J., Sen, S., Sweeney, H. L., Discher, D. E., *Cell* 2006, *126*, 677–689.

[84] Lo, C. M., Wang, H. B., Dembo, M., Wang, Y. L., *Biophys. J.* 2000, *79*, 144–152.

[85] Sundararaghavan, H. G., Monteiro, G. A., Firestein, B. L., Shreiber, D. I., *Biotechnol. Bioeng.* 2009, *102*, 632–643.

[86] Barkefors, I., Le Jan, S., Jakobsson, L., Hejll, E., Carlson, G., Johansson, H., Jarvius, J., Park, J. W., Jeon, N. L., Kreuger, J., *J. Biol. Chem.* 2008, *283*, 13905–13912.

[87] Gerhardt, H., Golding, M., Fruttiger, M., Ruhrberg, C., Lundkvist, A., Abramsson, A., Jeltsch, M., Mitchell, C., Alitalo, K., Shima, D., Betsholtz, C. J., *J. Cell Biol.* 2003, *161*, 1163–1177.

[88] Burdick, J. A., Khademhosseini, A., Langer, R., *Langmuir* 2004, *20*, 5153–5156.

[89] Du, Y., Hancock, M. J., He, J., Villa-Uribe, J. L., Wang, B., Cropek, D. M., Khademhosseini, A., *Biomaterials* 2010, *31*, 2686–2694.

[90] Vickerman, V., Blundo, J., Chung, S., Kamm, R., *Lab Chip* 2008, *8*, 1468–1477.

[91] Chung, S., Sudo, R., Mack, P. J., Wan, C. R., Vickerman, V., Kamm, R. D., *Lab Chip* 2009, *9*, 269–275.

[92] Hao, N., Yildirim, N., Wang, Y., Elston, T. C., Dohlman, H. G., *J. Biol. Chem.* 2003, *278*, 46506–46515.

[93] Madden, K., Snyder, M., *Annu. Rev. Microbiol.* 1998, *52*, 687–744.

[94] Moore, T. I., Chou, C. S., Nie, Q., Jeon, N. L., Yi, T. M., *PLoS One* 2008, *3*, e3865.

[95] Paliwal, S., Iglesias, P. A., Campbell, K., Hilioti, Z., Groisman, A., Levchenko, A., *Nature* 2007, *446*, 46–51.

[96] Burger, J., Gaines, K. F., Gochfeld, M., *Risk Anal.* 2001, *21*, 533–544.

[97] Jones, M. M., Cherian, M. G., *Toxicology* 1990, *62*, 1–25.

[98] Mahto, S. K., Yoon, T. H., Shin, H., Rhee, S. W., *Biomed. Microdevices* 2009, *11*, 401–411.

[99] Ye, N., Qin, J., Shi, W., Liu, X., Lin, B., *Lab Chip* 2007, *7*, 1696–1704.

[100] Kim, M. S., Yeon, J. H., Park, J. K., *Biomed. Microdevices* 2007, *9*, 25–34.

[101] Toh, Y. C., Lim, T. C., Tai, D., Xiao, G., van Noort, D., Yu, H., *Lab Chip* 2009, *9*, 2026–2035.

[102] Ling, Y., Rubin, J., Deng, Y., Huang, C., Demirci, U., Karp, J. M., *Khademhosseini, A. Lab Chip* 2007, *7*, 756–762.

